BIOCHEMISTRY

 Volume 45, Number 9 March 7, 2006

Accelerated Publications

Protein Stability and Surface Electrostatics: A Charged Relationship†

Samantha S. Strickler, Alexey V. Gribenko, Alexander V. Gribenko, Timothy R. Keiffer, Jessica Tomlinson, Tracey Reihle, Vakhtang V. Loladze, and George I. Makhatadze*

Department of Biochemistry and Molecular Biology, Pennsylvania State University College of Medicine, Hershey, Pennsylvania 17033

Received January 4, 2006; Revised Manuscript Received January 25, 2006

ABSTRACT: Engineering proteins to withstand a broad range of conditions continues to be a coveted objective, holding the potential to advance biomedicine, industry, and our understanding of disease. One way of achieving this goal lies in elucidating the underlying interactions that define protein stability. It has been shown that the hydrophobic effect, hydrogen bonding, and packing interactions between residues in the protein interior are dominant factors that define protein stability. The role of surface residues in protein stability has received much less attention. It has been believed that surface residues are not important for protein stability particularly because their interactions with the solvent should be similar in the native and unfolded states. In the case of surface charged residues, it was sometimes argued that solvent exposure meant that the high dielectric of the solvent will further decrease the strength of the charge−charge interactions. In this paper, we challenge the notion that the surface charged residues are not important for protein stability. We computationally redesigned sequences of five different proteins to optimize the surface charge−charge interactions. All redesigned proteins exhibited a significant increase in stability relative to their parent proteins, as experimentally determined by circular dichroism spectroscopy and differential scanning calorimetry. These results suggest that surface charge−charge interactions are important for protein stability and that rational optimization of charge−charge interactions on the protein surface can be a viable strategy for enhancing protein stability.

The progress in understanding forces responsible for protein stability has been enormous, largely through the combination of experimental and theoretical approaches. The packing of the hydrophobic core, disulfide and salt bridges, hydrogen bonding, and intrinsic secondary structure propensities have been shown to stabilize protein structure (*1*−*4*). Coinciding with these findings has been the development of different approaches that optimize these interactions. These approaches have made strides despite the computational complexity of the problem and limited knowledge of the dynamic balance between structure and stability, but they have also encountered limitations (*5*). Rational protein design has been dominated by algorithms that optimize interactions in the protein core (*6*−*11*). Conversely, only few algorithms have been developed that focus on surface interactions (*12*, *13*). This is attributed to the long-standing belief that since residues on the surface of the native protein are exposed to the solvent, they are less, if at all, important for protein

† This work was supported by a grant from the National Science Foundation (MCB 0416746). S.S.S., J.T., T.R., and T.R.K. were supported by NSF REU summer fellowships.

* To whom correspondence should be addressed: Department of Biochemistry and Molecular Biology, Pennsylvania State University College of Medicine, 500 University Dr., Hershey, PA 17033. E-mail: makhatadze@psu.edu. Phone: (717) 531-0712. Fax: (717) 531-7072.

10.1021/bi0600143 CCC: $33.50
Published on Web 02/07/2006

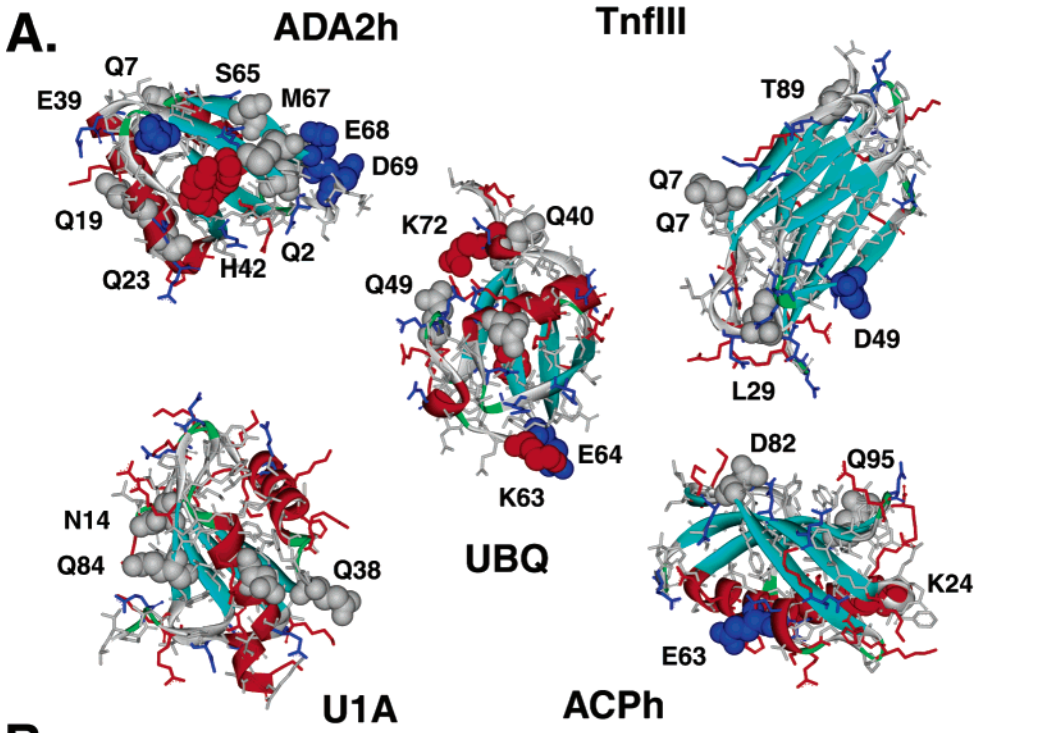

B.

```
                                1         2         3         4         5         6         7         8         9
                      123456789012345678901234567890123456789012345678901234567890123456789012345678901234567890
UBQ                   LQIFAKTLTGKTITLEVESSDTIDNVKSKIQDKEGIPPDQQKLIFAGKQLEDGKTLSDYNIQKESTLHLVLKLKGG
UBQ-6                 LQIFAETLTGKTITLEVESSDTIDNVKSKIQDKEGIPPDQQKLIFAGKQLEDGKTLSDYNIQKESTLHLVLKLKGG
UBQ-72                LQIFAKTLTGKTITLEVESSDTIDNVKSKIQDKEGIPPDQQKLIFAGKQLEDGKTLSDYNIQKESTLHLVLELKGG
UBQ-6/72              LQIFAETLTGKTITLEVESSDTIDNVKSKIQDKEGIPPDQQKLIFAGKQLEDGKTLSDYNIQKESTLHLVLELKGG
UBQ-GA#1              LQIFAKTLTGKTITLEVESSDTIDKVKSKIQDKEGIPPDKQKLIFAGKELEDGKTLSDYNIQKESTLQLVLELKGG
UBQ-GA#2              LQIFAKTLTGKTITLEVESSDTIDNVKSKIQDKEGIPPDQQKLIFAGKQLEDGKTLSDYNIQEKSTLELVLELKGG
UBQ-GA#3              LQIFAKTLTGKTITLEVESSDTIDKVKSKIQDKEGIPPDKQKLIFAGKELEDGKTLSDYNIQEKSTLELVLELKGG

ADA2h                 DQVLEIVPSNEEQIKNLLQLEAQEHLQLDFWKSPTTPGETAHVRVPFVNVQAVKVFLESQGIAYSIMIEDVQ
ADA2h-GA#1            DEVLEIVPSNEEQIKNLLQLEAQEHLQLDFWKSPTTPGETAEVRVPFVNVQAVKVFLESQGIAYKIKIEKVQ
ADA2h-GA#2            DQVLEIVPSNEEQIKNLLELEAKEHLQLDFWESPTTPGKTAHVRVPFVNVQAVKVFLESKGIAYKIMIKDVQ

TfnIII                RLDAPSQIEVKDVTDTTALITWFKPLAEIDGIELTYGIKDVPGDRTTIDLTEDENQYSIGNLKPDTEYEVSLISRRGDMSSNPAKETFTTGL
TfnIII-GA#1           RLDAPSKIEVKDVTDTTAKITWFKPLAEIDGIELTYGIKDVPGDRTTIKLTEDENQYSIGNLKPDTEYEVSLISRRGDMSSNPAKETFKTGA

ACPh                  AEGNTLISVDYEIFGKVQGVFFRKHTQAEGKKLGLVGWVQNTDRGTVQGQLQGPISKVRHMQEWLETRGSPKSHIDKANFNNEKVILKLDYSDFQIVK
ACPh-GA#1             AEGNTLISVDYEIFGKVQGVFFREHTQAEGKKLGLVGWVQNTDRGTVQGQLQGPISKVRHMQKWLETRGSPKSHIDKANFNKEKVILKLDYSDFKIVK

U1A                   AVPETRPNHTIYINNLNEKIKKDELKKSLYAIFSQFGQILDILVSRSLKMRGQAFVIFKEVSSATNALRSMQGFPFYDKPMRIQYAKTDSDIIAKMKGTF
U1A-GA#1              AVPETRPNHTIYIENLNEKIKKDELKKSLYAIFSQFGEILDILVSRSLKMRGQAFVIFKEVSSATEALRSMQGFPFYDKPMRIKYAKTDSDIIAKMKGTF
```

FIGURE 1: Structures and sequences of proteins. (A) Cartoon representation of the three-dimensional structures (PDB entry 1aye for ADA2h, PDB entry 1ubq for UBQ, PDB entry 1ten for TnfIII, PDB entry 1urn for U1A, and PDB entry 2acy for ACPh). The sites of substitutions are shown in CPK representation and color-coded to show basic (red) or acidic (blue) residues in the wild-type sequence. (B) Sequence alignment of the wild-type and designed proteins. The sites of substitutions are shown with bold red characters and are underlined.

stability. In the case of surface charged residues, as it was sometimes argued, solvent exposure also means that the high dielectric of the solvent will decrease the strength of the charge−charge interactions and thus lead to a further decrease in the contribution of these residues to protein stability (*5*). This notion was questioned several years ago when several groups demonstrated experimentally the importance of surface charge−charge interactions for protein stability (*13*−*22*). Furthermore, it became apparent that various computational models are capable of predicting the effects of single-site substitutions in the charged residues on the stability of several proteins (*13*, *15*, *16*, *20*, *22*−*25*). These observations led to the proposal that optimization of the surface charge−charge interactions can be a viable strategy for enhancing protein stability (*26*).

Here we provide an experimental test of whether computational optimization of charge−charge interactions on the protein surface can lead to an increase in the overall stability. For this we chose five different proteins, four of which were not studied in this laboratory before: ubiquitin (UBQ),[1] the activation domain of human procarboxypeptidase A2 (ADA2h), the fibronectin type III domain of human tenascin (TnfIII), human acylphosphatase (ACPh), and the N-terminal RNA-binding domain of human U1A protein (U1A). These proteins differ in size (there are 72, 76, 92, 98, and 100 amino acid residues in the sequences of ADA2h, UBQ, TnfIII, ACPh, and U1A, respectively) and in tertiary fold topology (Figure 1A).

MATERIALS AND METHODS

Proteins: Cloning, Expression, Purification, and Characterization. Each gene was synthetically constructed using

[1] Abbreviations: UBQ, ubiquitin; ADA2h, activation domain of human procarboxypeptidase A2; TnfIII, fibronectin type III domain of human tenascin; ACPh, human acylphosphatase; U1A, N-terminal RNA-binding domain of human U1A protein; CD, circular dichroism spectroscopy; GA, genetic algorithm.

a stepwise polymerase chain reaction (PCR) and cloned into the pGia expression vector under the control of the T7 promoter (*27*). Proteins had N-terminal six-His tags that could be removed either by CNBr treatment (ubiquitin and APCh) or by treatment with TEV protease (ADA2h and TNfIII). Proteins were expressed and purified using a standard protocol (*28*). The concentrations of the proteins were determined spectrophotometrically using the following extinction coefficients: $E^{1cm}_{1M,280nm} = 1280$ for ubiquitin, $E^{1cm}_{1M,280nm} = 69\,710$ for ADA2h, $E^{1cm}_{1M,280nm} = 9530$ for TnfIII, $E^{1cm}_{1M,280nm} = 5120$ for U1A, and $E^{1cm}_{1M,280nm} = 13\,940$ for ACPh. Final protein preparations were characterized using MALDI-TOF (Voyager DE-PRO, Perseptive Biosystems). In all cases, a single major peak was observed with a mass within 2−5 Da of that expected on the basis of the amino acid sequence of the parental and designed proteins (see Table S1 of the Supporting Information). Sedimentation equilibrium experiments were performed on a Beckman XLA analytical ultracentrifuge. Absorbance was monitored at 280 nm in long column cells, and samples were allowed to equilibrate at three different rotor speeds. Analysis of the analytical ultracentrifugation profiles was done globally as previously described (*27*).

Circular Dichroism (CD) Spectroscopy. All CD measurements were carried out on a JASCO J-715 spectropolarimeter. Far- and near-UV spectra were acquired in triplicate at 20 °C using quartz 1 and 10 mm thermostated cylindrical cuvettes, respectively. Protein concentrations were 0.2 mg/mL for far-UV spectra and 1−2 mg/mL for near-UV spectra. Urea-induced unfolding experiments were performed in 5 mM sodium acetate (pH 5.5) by monitoring the changes in ellipticity at 222 nm as described previously (*28*). Analysis of the data was done according to the linear extrapolation model using nonlinear regression routines as described previously (*28*). For temperature-induced unfolding, the ellipticity as a function of temperature was monitored at 222 nm for ADA2h and ACPh proteins and at 230 nm for TnfIII proteins in 1 cm quartz cuvettes. The protein concentration was 5 μM for all samples. Analysis of the data was done according to a two-state model as described previously (*29*).

Differential Scanning Calorimetry (DSC). All DSC experiments were conducted on a VP-DSC instrument (Microcal Inc., Northhampton, MA) at a scan rate of 90 deg/h. Protein concentrations were ∼1 mg/mL in 50 mM sodium phosphate (pH 7.0). Melted samples were cooled and reheated to analyze reversibility. For all studied proteins, the reversibility was found to be better than 90%. Analysis of the heat capacity profiles was done using a two-state model as described previously (*29*).

Calculation of the Energies of Surface Charge−Charge Interactions. The energies of charge−charge interactions, ΔG_{q-q}, were calculated as described previously (*28*, 29) (see also the Supporting Information). The structures of all designed proteins were modeled using the known structures of the corresponding wild-type proteins using Modeler version 7.7 (*30*). To assess the errors in the calculated energies of charge−charge interactions, 11 different structures were generated, individual calculations were performed on each of these 11 structures, and averaged values with the mean standard deviations are shown. In all calculations, it was assumed that there were no residual charge−charge interactions in the unfolded state. This assumption is not always valid for quantitative analysis (*31*−*35*), but theoretical calculations suggest that the charge−charge interactions in the unfolded state are usually relatively weak (*24*, *36*, *37*) and thus should not dramatically affect the more qualitative analysis presented here.

RESULTS AND DISCUSSION

The energies of charge−charge interactions were calculated using several computational models, all of which led to similar results (see Materials and Methods). For the search of the sequences with optimized charge−charge interactions, we used the genetic algorithm (GA) (*38*). In our implementation of this algorithm, each set of charge distributions is considered to be a chromosome. These chromosomes are allowed to undergo mutations (i.e., change of the charged state of individual residues) or crossover (i.e., exchange parts of chromosomes). At each step, chromosomes are retained if their energy of charge−charge interactions is better than a preset cutoff value. Evolutionary pressure is kept in a form of energy penalty for each mutation introduced into a chromosome. For each protein, the relative accessibility of all residues to the solvent was calculated and those with side-chain accessibility higher than 50% were considered for optimization, except for the residues with side chains forming multiple hydrogen bonds. The GA provided numerous sequence energies of charge−charge interactions that were more favorable, relative to those of the wild-type sequence (Figure S1 of the Supporting Information). Thus, the sequences with the largest increase in energy due to the fewest number of substitutions were selected. From these sequences, several were selected for experimental validation. Sequence alignment of wild-type and designed proteins is shown in Figure 1B. Figure 2 compares the energies of charge−charge interactions to emphasize the optimization strategies (see also Figures S2 and S3 of the Supporting Information).

Three different variants of ubiquitin (see Figure 1B for sequences) were tested experimentally. The first ubiquitin variant includes one charge reversal, one charge neutralization, and three new charges in place of previously uncharged polar positions. The second ubiquitin variant had four substitutions, all of which were charge reversals, while the third sequence combined the second sequence with the three new charges of the first sequence. Two variants of the α/β sandwich protein ADA2h were constructed. One variant had five substitutions relative to the wild type, of which two were charge reversals and three introduced new charge−charge interaction sites. The second variant had seven substitutions, of which three were charge reversals and four were new charged positions. New charges in both variants of ADA2h were introduced in place of uncharged polar side chains. One variant was tested for the all β-sheet protein TfnIII. In this variant, there were four substitutions relative to the wild-type protein, of which one residue underwent a charge reversal and three charged residues were introduced at previously uncharged polar and nonpolar positions. The designed variant of the human acylphosphatase, ACPh, had four substitutions. Again, charges were reversed and new charges introduced. The largest protein that was tested was U1A, in which all four substitutions introduced charged residues at previously uncharged polar positions in the

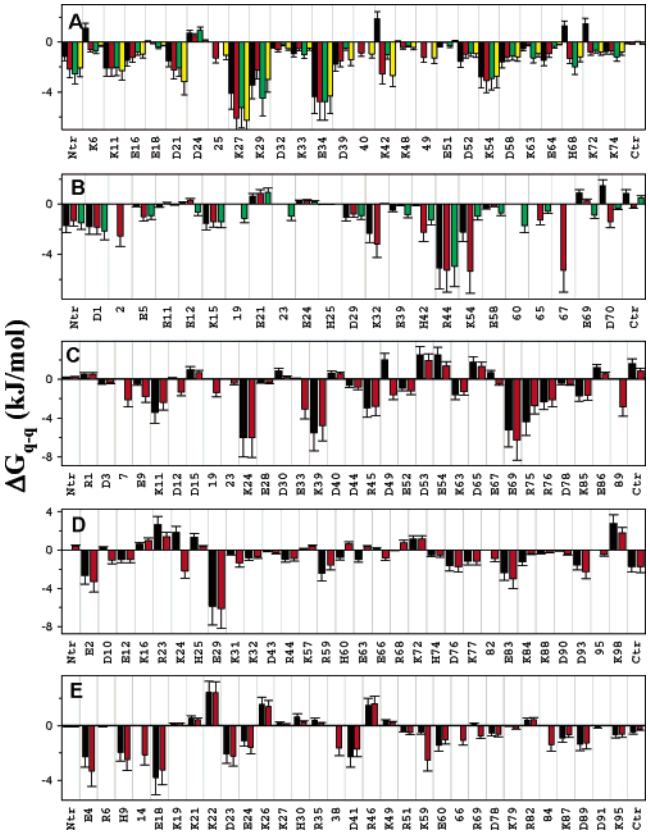

FIGURE 2: Comparison of the energies of charge−charge interactions in the wild-type and designed sequences: (A) UBQ, (B) ADA2h, (C) TnfIII, (D) ACPh, and (E) U1A. Each bar corresponds to the total energy of charge−charge interactions of that residue with all other ionizable residues in the protein. Black bars are for the wild-type proteins, and red and green (in panels A and B) bars are for the GA-designed variants. Error bars are calculated as described in Materials and Methods.

sequence. Once this had been done, the unfavorable interactions existing in the wild-type structure remained unperturbed. Therefore, the overall changes in the charge−charge interactions arise solely from the addition of newly added charged residues (Figure 2).

Structural properties of each parental and engineered protein were characterized by circular dichroism spectroscopy. Both far- and near-UV CD spectra of parental and engineered proteins were similar, illustrating that the substitutions did not have a significant effect on the protein structure (see Figure S4 of the Supporting Information). Analytical ultracentrifugation experiments were carried out to eliminate the possibility that changes in oligomerization state are responsible for the observed changes in stability. Analysis revealed that all proteins remain monomeric under experimental conditions (see Figure S5 of the Supporting Information). Therefore, the observed differences in thermodynamic parameters cannot be attributed to changes in the structure or in the oligomerization state of the engineered proteins.

Thermodynamic stabilities of the parent and designed proteins were compared using temperature- or denaturant-induced unfolding using differential scanning calorimetry and/or circular dichroism spectroscopy. The following results were obtained (Figure 3).

UBQ. Temperature-induced unfolding of ubiquitin at pH >5 is irreversible, and therefore, stability was measured using urea-induced unfolding monitored by following the changes in ellipticity at 222 nm using CD. Analysis of the unfolding profile for the reference protein gives a ΔG of 9.6 kJ/mol at 25 °C. The stability of all three designed ubiquitin variants (Figure 3A) is significantly higher than that of the parent protein, with UBQ-GA#2 and UBQ-GA#3 variants being 18.6 and 17.4 kJ/mol more stable, respectively. Such a dramatic increase in stability due to the substitutions at the surface positions is rather impressive, keeping in mind that the contributions of other interactions that were affected by the substitutions were not taken into account in the calculations. The increase in stability is much greater than the increase in stability upon removal of just one or two unfavorable interactions such as, for example, K6E, K72E, or K6E/K72E variants (Figure 3A), which lead to increases in the Gibbs free energy of unfolding ($\Delta\Delta G$) of 3.3, 1.7, and 5.2 kJ/mol, respectively (Figure 3F).

U1A. Temperature-induced unfolding of U1A at neutral pH is irreversible, and therefore, the stabilities of the wild-type and designed U1A proteins were assessed by urea-induced unfolding, monitored by far-UV CD (222 nm) (Figure 3B). Analysis of the unfolding profile of the wild-type U1A protein gives a ΔG of 25.1 kJ/mol, a value comparable with previous estimates from GdmHCl-induced unfolding (*39*). The designed U1A variant unfolds at a higher urea concentration, which translates into a 4.1 kJ/mol increase in the thermodynamic stability of the designed U1A (Figure 3F).

ADA2. From the comparison of the far-UV CD melting profiles for the wild type and two variants of ADA2h, it is clear that the redesigned ADA2h proteins have an increased stability (Figure 3C). For the wild type, the T_m was 66.9 °C. The redesigned ADA2h-GA#1 produced an increase in T_m of ∼3 °C (69.8 °C). A more dramatic increase in stability was observed for the ADA2h-GA#2 protein, which had a T_m of 76.7 °C, nearly 10 °C greater than that of the wild type. These changes in T_m translate into increases in the thermodynamic stability of the designed variants of 4.1 and 10.7 kJ/mol at 25 °C, respectively (Figure 3F).

ACPh. Stabilities of the ACPh proteins were determined using thermal denaturation monitored by DSC (Figure 3D) or far-UV CD (not shown). Thermodynamic parameters derived from the analysis of the profiles for the wild-type ACPh are in excellent agreement with the previously reported values (*40*). Comparison of the wild type and designed variant shows that the ACPh variant is 5.4 °C more stable which translates into a 7 kJ/mol greater thermodynamic stability at 25 °C (Figure 3F).

TfnIII. The stability of the parental and variant TfnIII proteins was measured using temperature-induced unfolding monitored by DSC (Figure 3E) or far-UV CD (not shown). Analysis of the DSC and CD experiments gives similar transition temperatures of unfolding; that for the wild type (56.4 °C) is identical to those previously reported (*41*). The redesigned variant, TfnIII-GA#1, has a T_m of 66 °C, a nearly 10 °C increase in stability compared to that of the parental protein, which corresponds to an increase in the thermodynamic stability of the designed protein of 5.4 kJ/mol at 25 °C (Figure 3F).

We have thus redesigned the surface charge−charge interactions in five different proteins ranging in size from 72 to 100 amino acid residues and having vastly different

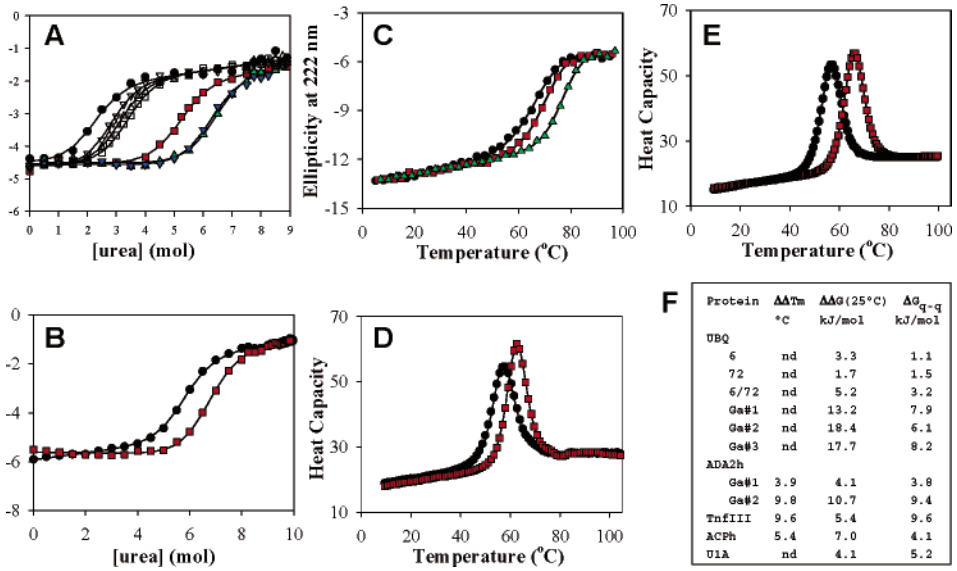

F

Protein	ΔΔTm °C	ΔΔG(25°C) kJ/mol	ΔG_{q-q} kJ/mol
UBQ			
6	nd	3.3	1.1
72	nd	1.7	1.5
6/72	nd	5.2	3.2
Ga#1	nd	13.2	7.9
Ga#2	nd	18.4	6.1
Ga#3	nd	17.7	8.2
ADA2h			
Ga#1	3.9	4.1	3.8
Ga#2	9.8	10.7	9.4
TnfIII	9.6	5.4	9.6
ACPh	5.4	7.0	4.1
U1A	nd	4.1	5.2

FIGURE 3: Comparison of stabilities of the wild type and designed variants of studied proteins. Symbols are for the experimental measured parameters, and solid lines show the results of a fit to a two-state model. (A) Urea-induced unfolding of UBQ variants as monitored by changes in ellipticity at 222 nm: (●) UBQ, (△) UBQ-6, (▽) UBQ-72, (□) UBQ-6/72, (red squares) UBQ-GA#1, (green triangles) UBQ-GA#2, and (blue inverted triangles) UBQ-GA#3. (B) Urea-induced unfolding of U1A variants as monitored by changes in ellipticity at 222 nm: (●) U1A and (red squarees) U1A-GA#1. (C) Temperature-induced unfolding of ADA2h variants as monitored by changes in ellipticity at 222 nm: (●) ADA2h, (red squares) ADA2h-GA#1, and (green triangles) ADA2h-GA#2. (D) Temperature-induced unfolding of ACPh variants as monitored by DSC: (●) ACPh and (red squares) ACPh-GA#1. (E) Temperature-induced unfolding of TnfIII variants as monitored by DSC: (●) TnfIII and (red squares) TnfIII-GA#1. (F) Comparison of stabilities of the wild type and designed variants of studied proteins. $\Delta\Delta T_m$ and $\Delta\Delta G$ (25 °C) are the experimentally determined changes in transition temperature and Gibbs energy, respectively, and ΔG_{q-q} is the energy change of charge−charge interactions relative to the wild-type protein (nd, not determined).

secondary structures and three-dimensional topologies. In all cases, an increase in stability was observed. Successful stabilization of ubiquitin, ADA2h, TfnIII, ACPh, and U1A described here and engineering of the CspB protein reported previously (*29*) suggest that optimization of surface charges is a simple and consistently reliable approach to increasing protein stability. As exemplified by these redesigned proteins, the approach has an inherent plasticity. It can be applied to a wide range of proteins that have various folds, topologies, and secondary structures. In addition, charge redistribution can be accomplished through multiple strategies. Basic charges may be changed to acidic charges, and vice versa as with ubiquitin. In addition, the introduction of new charges is a viable method of increasing protein stability, whether it is in conjunction with charge reversals as with ADA2h, TfnIII, and ACPh or independently as with U1A. The optimization of charges in ubiquitin and ADA2h also accentuates that there are multiple arrangements of charges, which may be employed to increase a protein's stability. This flexibility may prove to be invaluable, allowing for the conservation of special properties such as residues around the active site when enzymes are redesigned.

Results reported here thus support two major points. (1) Surface charge−charge interactions are important for protein stability. (2) The surface charge−charge interactions can be redesigned in a rational way to manipulate protein stability. The energetics of charge−charge interactions on the protein surface can be qualitatively well predicted using a number of different computational models. The computational tractability is very promising not only for the protein engineering field but also from a fundamental perspective, suggesting that significant progress has already been achieved. It does not mean, however, that we understand charge−charge interactions in sufficient detail for quantitative predictions about the thermodynamics. The energetic consequences of the interactions between charges and protein dipoles are still unclear, as is the role of conformational flexibility in both native and unfolded states, how ions influence the strength of both short-range and long-range charge−charge interactions, and what the role of interactions of surface charges with the solvent water is (*42*−*45*). Incorporation of all these effects into a single computational algorithm will undoubtedly have broad applications for the rational design of thermostable proteins.

ACKNOWLEDGMENT

We thank Dr. Kathleen Hall for providing the U1A gene.

SUPPORTING INFORMATION AVAILABLE

Results of circular dichroism and analytical ultracentrifugation experiments, details of calculations of charge−charge interactions using different computational models, and a description of the optimization algorithm. This material is available free of charge via the Internet at http://pubs.acs.org.

REFERENCES

1. Baldwin, E. P., and Matthews, B. W. (1994) Core-packing constraints, hydrophobicity and protein design, *Curr. Opin. Biotechnol. 5*, 396−402.
2. Fersht, A., and Winter, G. (1992) Protein engineering, *Trends Biochem. Sci. 17*, 292−295.
3. Makhatadze, G. I., and Privalov, P. L. (1995) Energetics of protein structure, *Adv. Protein Chem. 47*, 307−425.
4. Pace, C. N., Shirley, B. A., McNutt, M., and Gajiwala, K. (1996) Forces contributing to the conformational stability of proteins, *FASEB J. 10*, 75−83.
5. Schueler-Furman, O., Wang, C., Bradley, P., Misura, K., and Baker, D. (2005) Progress in modeling of protein structures and interactions, *Science 310*, 638−642.

6. Mendes, J., Guerois, R., and Serrano, L. (2002) Energy estimation in protein design, *Curr. Opin. Struct. Biol. 12*, 441−446.
7. Park, S., Yang, X., and Saven, J. G. (2004) Advances in computational protein design, *Curr. Opin. Struct. Biol. 14*, 487−494.
8. DeGrado, W. F., Summa, C. M., Pavone, V., Nastri, F., and Lombardi, A. (1999) De novo design and structural characterization of proteins and metalloproteins, *Annu. Rev. Biochem. 68*, 779−819.
9. Street, A. G., and Mayo, S. L. (1999) Computational protein design, *Struct. Folding Des. 7*, R105−R109.
10. Pokala, N., and Handel, T. M. (2001) Review: Protein design−where we were, where we are, where we're going, *J. Struct. Biol. 134*, 269−281.
11. Dantas, G., Kuhlman, B., Callender, D., Wong, M., and Baker, D. (2003) A large scale test of computational protein design: Folding and stability of nine completely redesigned globular proteins, *J. Mol. Biol. 332*, 449−460.
12. Villegas, V., Viguera, A. R., Aviles, F. X., and Serrano, L. (1996) Stabilization of proteins by rational design of α-helix stability using helix/coil transition theory, *Folding Des. 1*, 29−34.
13. Marshall, S. A., Morgan, C. S., and Mayo, S. L. (2002) Electrostatics significantly affect the stability of designed homeodomain variants, *J. Mol. Biol. 316*, 189−199.
14. Grimsley, G. R., Shaw, K. L., Fee, L. R., Alston, R. W., Huyghues-Despointes, B. M., Thurlkill, R. L., Scholtz, J. M., and Pace, C. N. (1999) Increasing protein stability by altering long-range coulombic interactions, *Protein Sci. 8*, 1843−1849.
15. Loladze, V. V., Ibarra-Molero, B., Sanchez-Ruiz, J. M., and Makhatadze, G. I. (1999) Engineering a thermostable protein via optimization of charge−charge interactions on the protein surface, *Biochemistry 38*, 16419−16423.
16. Spector, S., Wang, M., Carp, S. A., Robblee, J., Hendsch, Z. S., Fairman, R., Tidor, B., and Raleigh, D. P. (2000) Rational modification of protein stability by the mutation of charged surface residues, *Biochemistry 39*, 872−879.
17. Perl, D., Mueller, U., Heinemann, U., and Schmid, F. X. (2000) Two exposed amino acid residues confer thermostability on a cold shock protein, *Nat. Struct. Biol. 7*, 380−383.
18. Koide, A., Jordan, M. R., Horner, S. R., Batori, V., and Koide, S. (2001) Stabilization of a fibronectin type III domain by the removal of unfavorable electrostatic interactions on the protein surface, *Biochemistry 40*, 10326−10333.
19. Lee, K. K., Fitch, C. A., and Garcia-Moreno, E. B. (2002) Distance dependence and salt sensitivity of pairwise, coulombic interactions in a protein, *Protein Sci. 11*, 1004−1016.
20. Schwehm, J. M., Fitch, C. A., Dang, B. N., Garcia-Moreno, E. B., and Stites, W. E. (2003) Changes in stability upon charge reversal and neutralization substitution in staphylococcal nuclease are dominated by favorable electrostatic effects, *Biochemistry 42*, 1118−1128.
21. Permyakov, S. E., Makhatadze, G. I., Owenius, R., Uversky, V. N., Brooks, C. L., Permyakov, E. A., and Berliner, L. J. (2005) How to improve nature: Study of the electrostatic properties of the surface of α-lactalbumin, *Protein Eng., Des. Sel. 18*, 425−433.
22. Lee, C. F., Makhatadze, G. I., and Wong, K. B. (2005) Effects of Charge-to-Alanine Substitutions on the Stability of Ribosomal Protein L30e from *Thermococcus celer*, *Biochemistry 44*, 16817−16825.
23. Dominy, B. N., Perl, D., Schmid, F. X., and Brooks, C. L., III (2002) The effects of ionic strength on protein stability: The cold shock protein family, *J. Mol. Biol. 319*, 541−554.
24. Zhou, H. X., and Dong, F. (2003) Electrostatic contributions to the stability of a thermophilic cold shock protein, *Biophys. J. 84*, 2216−2222.
25. Laurents, D. V., Huyghues-Despointes, B. M., Bruix, M., Thurlkill, R. L., Schell, D., Newsom, S., Grimsley, G. R., Shaw, K. L., Trevino, S., Rico, M., Briggs, J. M., Antosiewicz, J. M., Scholtz, J. M., and Pace, C. N. (2003) Charge−charge interactions are key determinants of the p*K* values of ionizable groups in ribonuclease Sa (pI = 3.5) and a basic variant (pI = 10.2), *J. Mol. Biol. 325*, 1077−1092.
26. Sanchez-Ruiz, J. M., and Makhatadze, G. I. (2001) To charge or not to charge? *Trends Biotechnol. 19*, 132−135.
27. Gribenko, A. V., Hopper, J. E., and Makhatadze, G. I. (2001) Molecular characterization and tissue distribution of a novel member of the S100 family of EF-hand proteins, *Biochemistry 40*, 15538−15548.
28. Makhatadze, G. I., Loladze, V. V., Ermolenko, D. N., Chen, X., and Thomas, S. T. (2003) Contribution of surface salt bridges to protein stability: Guidelines for protein engineering, *J. Mol. Biol. 327*, 1135−1148.
29. Makhatadze, G. I., Loladze, V. V., Gribenko, A. V., and Lopez, M. M. (2004) Mechanism of thermostabilization in a designed cold shock protein with optimized surface electrostatic interactions, *J. Mol. Biol. 336*, 929−942.
30. Marti-Renom, M. A., Stuart, A. C., Fiser, A., Sanchez, R., Melo, F., and Sali, A. (2000) Comparative protein structure modeling of genes and genomes, *Annu. Rev. Biophys. Biomol. Struct. 29*, 291−325.
31. Cho, J. H., and Raleigh, D. P. (2005) Mutational Analysis Demonstrates that Specific Electrostatic Interactions can Play a Key Role in the Denatured State Ensemble of Proteins, *J. Mol. Biol. 353*, 174−185.
32. Trefethen, J. M., Pace, C. N., Scholtz, J. M., and Brems, D. N. (2005) Charge−charge interactions in the denatured state influence the folding kinetics of ribonuclease Sa, *Protein Sci. 14*, 1934−1938.
33. Oliveberg, M., Arcus, V. L., and Fersht, A. R. (1995) pK_a values of carboxyl groups in the native and denatured states of barnase: The pK_a values of the denatured state are on average 0.4 units lower than those of model compounds, *Biochemistry 34*, 9424−9433.
34. Kuhlman, B., Luisi, D. L., Young, P., and Raleigh, D. P. (1999) pK_a values and the pH dependent stability of the N-terminal domain of L9 as probes of electrostatic interactions in the denatured state. Differentiation between local and nonlocal interactions, *Biochemistry 38*, 4896−4903.
35. Pace, C. N., Alston, R. W., and Shaw, K. L. (2000) Charge−charge interactions influence the denatured state ensemble and contribute to protein stability, *Protein Sci. 9*, 1395−1398.
36. Elcock, A. H. (1999) Realistic modeling of the denatured states of proteins allows accurate calculations of the pH dependence of protein stability, *J. Mol. Biol. 294*, 1051−1062.
37. Zhou, H. X. (2002) A Gaussian-chain model for treating residual charge−charge interactions in the unfolded state of proteins, *Proc. Natl. Acad. Sci. U.S.A. 99*, 3569−3574.
38. Godoy-Ruiz, R., Perez-Jimenez, R., Garcia-Mira, M. M., Plaza del Pino, I. M., and Sanchez-Ruiz, J. M. (2005) Empirical parametrization of p*K* values for carboxylic acids in proteins using a genetic algorithm, *Biophys. Chem. 115*, 263−266.
39. Kranz, J. K., Lu, J., and Hall, K. B. (1996) Contribution of the tyrosines to the structure and function of the human U1A N-terminal RNA binding domain, *Protein Sci. 5*, 1567−1583.
40. Taddei, N., Chiti, F., Paoli, P., Fiaschi, T., Bucciantini, M., Stefani, M., Dobson, C. M., and Ramponi, G. (1999) Thermodynamics and kinetics of folding of common-type acylphosphatase: Comparison to the highly homologous muscle isoenzyme, *Biochemistry 38*, 2135−2142.
41. Clarke, J., Hamill, S. J., and Johnson, C. M. (1997) Folding and stability of a fibronectin type III domain of human tenascin, *J. Mol. Biol. 270*, 771−778.
42. Kumar, S., and Nussinov, R. (2002) Close-range electrostatic interactions in proteins, *ChemBioChem 3*, 604−617.
43. Honig, B., and Nicholls, A. (1995) Classical electrostatics in biology and chemistry, *Science 268*, 1144−1149.
44. Schutz, C. N., and Warshel, A. (2001) What are the dielectric "constants" of proteins and how to validate electrostatic models? *Proteins 44*, 400−417.
45. Garcia-Moreno, E. B., and Fitch, C. A. (2004) Structural interpretation of pH and salt-dependent processes in proteins with computational methods, *Methods Enzymol. 380*, 20−51.

BI0600143